Late killing of *Plasmodium berghei* in the liver by an anti-circumsporozoite protein monoclonal antibody

Manuela C. Aguirre-Botero [1], Olga Pacios [1,3], Susanna Celli [1], Eduardo Aliprandini [1,4], Anisha Gladston [1,2], Jean-Michel Thiberge [1], Pauline Formaglio [1,5] and Rogerio Amino [1, *]

[1] Institut Pasteur, Université Paris Cité, Malaria Infection and Immunity, BioSPC, F-75015, Paris, France

[2] Department of Life Sciences, Imperial College London, London SW7 2AZ, UK

[3] Current affiliation: Microbiology Department - A Coruña Hospital, MicroTM-INIBIC, A Coruña, Spain

[4] Current affiliation: Affinity Reagents Team, Biologics Engineering, AstraZeneca, Cambridge, UK

[5] Current affiliation : Sorbonne Université, Inserm U1135, CNRS ERL8255, Centre d'Immunologie et des Maladies Infectieuses (CIMI-Paris), 91 Boulevard de l'Hôpital, F-75013 Paris, France

* Correspondence: roti@pasteur.fr (R.A.)

Abstract: The transmission of *Plasmodium* parasites into the vertebrate host skin begins with the inoculation of a few sporozoites during the bite of an infected mosquito. This motile stage invades cutaneous blood vessels to reach the liver and infect hepatocytes. The first approved malaria vaccine RTS, S/AS01 elicits high titers of antibodies against the circumsporozoite protein (CSP), the main protein on the surface of sporozoites. Protection mainly unfolds during parasite migration through the host, but rare and potent protective antibodies can additionally neutralize sporozoite in the blood and liver. Here, using microscopy and bioluminescence imaging in a rodent malaria model, we show the dynamics of parasite elimination in the liver by the 3D11 anti-CSP monoclonal antibody (mAb) targeting the repetitive region of the *Plasmodium berghei* CSP. Our data confirmed that in passively immunized mice protection against an intravenous sporozoite challenge requires much higher concentrations of antibody than a cutaneous challenge adjusted to elicit the same level of infection. Sporozoite arrest in the liver was not affected by the protective antibody. A two-fold decrease in the crossing of the hepatic sinusoidal barrier was observed after three hours post sporozoite inoculation, associated with the loss of parasite motility. Intriguingly, the elimination of most parasites in the liver occurred after 5 hours post-inoculation, indicating a late action of this protective antibody. *In vitro*, 3D11 strongly inhibited the invasion of HepG2 cells by sporozoites in positive correlation with its cytotoxic activity. Additionally, this protective mAb impaired the intracellular development of liver stages, confirming the late cytotoxic effect of this antibody. Altogether, 3D11-mediated protection in the liver is mainly associated with its cytotoxic activity, which leads to the inhibition of sporozoite motility, sinusoidal extravasation, cell invasion, and to the killing inside the liver parenchyma.

Keywords: Malaria, *Plasmodium*, monoclonal antibodies

Introduction

Malaria remains the deadliest parasitic disease worldwide and is responsible every year for over 600, 000 deaths, mainly in sub-Saharan Africa [1]. The infection, caused by parasites of the genus *Plasmodium*, begins with the inoculation of the sporozoite stage into the skin by an infected mosquito [2]. Within the skin, sporozoites become activated and move through the dermis until some find and invade a blood vessel [3,4]. Upon entering circulation, parasites arrest in the liver [5], cross the sinusoidal barrier within 2-3 h [6] and eventually infect the hepatocytes. In there, they develop into the stages, giving rise after 48 – 52 h to erythrocyte-infecting stages which are ultimately released into the blood [7,8]. The sporozoite surface is covered by a dense coat of the immunodominant circumsporozoite protein (CSP) [9]. This protein has a highly conserved structural organization across diverse *Plasmodium* species, comprising conserved N- and C-terminal domains and a highly variable and repetitive central region. Due to its surface localization, conservation between the same species and immunodominant character, CSP has been used in the most effective malaria vaccines. For example, the RTS,S/AS01 and R21/Matrix M malaria vaccines, recommended by the World Health Organization (WHO), include a fragment of the central repetitive region and the C-terminal domain of the CSP from the human infecting *Plasmodium falciparum* (Pf) 3D7 strain [10]. Extensive research has demonstrated a positive correlation between high levels of anti-CSP antibodies (Abs) induced by the RTS,S/AS01 vaccine and its efficacy against malaria [11–13]. Remarkably, these Abs have proven to protect *in vivo* against malaria in various experimental settings, including, mice [14–21], monkeys [22,23], and humans [24–26].

Specifically, it has been observed that Abs that target the repetitive region exhibit a cytotoxic effect on the sporozoites, accompanied by the shedding of the CSP surface coat [14,27], inhibition of motility, loss of infectivity [28,29], and eventual parasite death [30,31]. All these effects seem to be independent of downstream host effectors like the complement and immune host cells [30]. Instead, Ab cytotoxicity was shown to increase in a 3D matrix mimicking the cutaneous environment [31]. Accordingly, neutralization of sporozoites by anti-CSP Abs occurs primarily during their migration through the skin [30,31] and is dependent on sporozoite motility and host cell wounding activities [30], which are both crucial for parasite progression in the dermis[32].

Yet, while the role of the skin in anti-CSP Abs-mediated sporozoite neutralization has been increasingly studied, little is known about the mechanisms by which these effectors contribute, outside of the skin, to sterilely protect against sporozoite infection. Potent Abs or high concentrations of them were shown to efficiently target sporozoites in the blood and liver (BL) following intravenous (i.v.) parasite inoculation which bypasses the skin [15,21,31]. In this study, we analyzed how 3D11, a monoclonal Ab (mAb) against the CSP against *P. berghei* (Pb) that has been shown to inhibit parasite motility and kill sporozoites *in vitro* [30], as well as to inhibit motility in the skin [33], affects sporozoite distribution in the BL, hepatocyte infection and intracellular development. The current investigation provides a comprehensive view of the kinetics and mode of action of 3D11 on multiple steps of liver infection.

Results

Tissue-dependent neutralization of Pb sporozoites

To assess how efficiently the anti-PbCSP repeat mAb 3D11 targets sporozoites in the skin and in the BL, mice were passively immunized intraperitoneally with 100 µg of mAb 3D11 or with an isotype control (W24). Twenty-four hours later, animals were challenged either i.v. or micro-injected into the skin with respectively 1,000 and 5,000 GFP-expressing sporozoites. The sporozoite inoculum was adjusted to achieve comparable infection regardless of the route of parasite injection, as reflected by the quantification of parasitemia measured by the percentage of infected red blood cells (Figure 1A). In addition, we compared the results obtained following these two routes of inoculation with infection initiated by sporozoites naturally transmitted by mosquitos. The extent of bite exposure was adjusted to reach a level of host infection similar to the previously described skin and i.v. Protection was assessed by measuring the parasitemia 5 days after sporozoite inoculation when parasites are growing exponentially in the blood (Figure 1A). Sterile protection was defined as the percentage of uninfected animals ten days after the challenge (Figure 1B). Altogether, the skin and the bite challenge allowed us to study 3D11 neutralizing activity in the cutaneous tissue as well as in the BL, while the i.v. challenge bypasses the skin, and reflects only the mAb-neutralizing activity in the BL.

Passive transfer of 100 µg of mAb 3D11 sterilely protected animals only when sporozoites were inoculated into the skin, either by micro-injection (100%) or by mosquito bite (86%, Figure 1A, B). Despite not eliciting sterile protection, 3D11 led to a 10-fold reduction in parasitemia after i.v. challenge (Figure 1A), and accordingly, a delayed prepatency in passively immunized mice compared to the control group (Figure 1B). These results confirm that the skin challenge more closely resembles the mosquito bite challenge than the i.v. challenge, as previously observed [30,31]. Furthermore, we confirmed that 3D11 predominantly neutralizes sporozoites in the skin, but also targets sporozoites in the BL [33].

Next, we investigated the impact of higher mAb concentration on sporozoite neutralization in the BL. Following the same passive immunization schedule, we compared the parasitemia of mice injected intraperitoneally with 100 and 300 µg of mAb 3D11 and challenged i.v. 24 h later. Increasing the mAb dose to 300 µg further reduced the parasitemia by ~100-fold compared to the control (Figure 1C). However, this 3-fold increase of the mAb dose still failed to confer sterile protection against i.v. challenge while 100 µg of 3D11 were sufficient to clear the infection in 86-100% of the mice after skin or bite challenge (Figure 1A, C). These results indicate that 3D11 sporozoite neutralization in the BL is concentration-dependent but is not as efficient as in the skin.

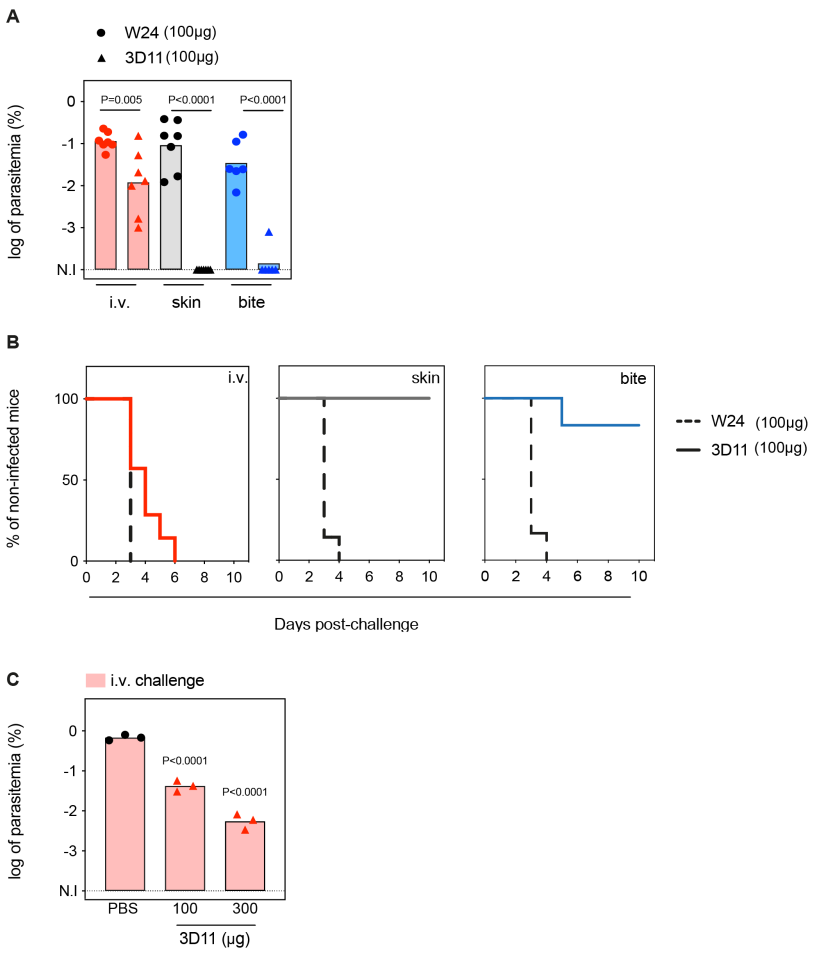

Figure 1. Tissue-dependent neutralization of Pb sporozoites. (A) Comparison of the log parasitemia at day 5 post-challenge and **(B)** survival curves of animals that received 100 µg of the isotype control (W24) or 3D11 mAb followed by i.v. inoculation of sporozoites, in the skin or by mosquito bite (bite). For i.v. and skin n=7 mice. For mosquito bite n=6 mice. N.I: non-infected. **(C)** Titration of the protection elicited by 3D11 after the i.v. challenge, 24 h after intraperitoneal transfer of the antibody (n =3). **(A, C)** Statistical significance was determined by one-way ANOVA with Holm-Šídák correction for multiple comparisons.

Kinetics of Pb sporozoite elimination in the liver

To further characterize 3D11 sporozoite neutralization in the BL, we first quantified the biodistribution and elimination of parasites in the mouse body by bioluminescence imaging following infection with sporozoites constitutively expressing a GFP-luciferase fusion protein. By comparing parasite load in 3D11 and PBS-treated mice at four critical time points covering almost all the parasite hepatic life cycle (Figure 2A), we measured the potential of 3D11 to (i) kill parasites in the blood, (ii) inhibit the specific arrest of sporozoites in the liver, and (iii) hinder their intracellular development.

For the quantification of parasite load in the hepatic tissue, the body of each animal was divided into four regions of interest (ROI), and the bioluminescent signal emanating from the upper abdominal ROI was attributed to the liver (Figure 2B) [5]. Mice were injected with PBS or 100 µg of 3D11 i.v to maximize mAb transfer into the blood circulation. Bioluminescence distribution in the mouse body was

then measured 7 min after parasite inoculation to quantify the specific arrest of sporozoites in the liver [5]. By calculating the ratio between the total flux of photons in the hepatic ROI and the total flux in the whole body over 5 min acquisition (Figure 2B), we estimated the percentage of parasites accumulating in the liver between 7-12 min after sporozoite injection (Figure 2B, left: control, right: 3D11-treated mouse). The total flux and the percentage of signal in the liver were not affected by the presence of 3D11 (83% for control vs. 87% for 3D11-treated mice p=0.36, Figure 2C and 2D, 7 min), indicating that 3D11 neither significantly killed parasites at this early time point of infection nor affected sporozoite arrest in the liver.

Bioluminescence was further measured in the same animals 4, 24, 44 h (Figure 2), and 72 h (Figure S1) later. Since most sporozoites cross the liver sinusoidal barrier within 3 h post-i.v. inoculation [6,34], the bioluminescent signal acquired in the hepatic region at 4 h in the control group should correspond to sporozoites inside the liver parenchyma, while between 24 and 44 h, the signal should reflect the development of exoerythrocytic forms within the hepatocytes (Figure 2A). At 4 h, the difference between the 3D11- and the vehicle-treated group was ~2-fold but it was not statistically different, while at 24 h around a ~40-fold decrease in the signal was evident (p=0.008, Figure 2D and E). This decrease from the treated compared to the control group was maintained between 24h and 44 h and then later in the blood at 72 h (Figure 2D, Figure S1), suggesting that there is no further effect of 3D11 mAb on late liver and blood stages. Altogether, these data indicate that 3D11 rather than having an early effect on sporozoites, e.g. in the homing or killing in the blood, requires more than 4 h to eliminate most parasites in the liver.

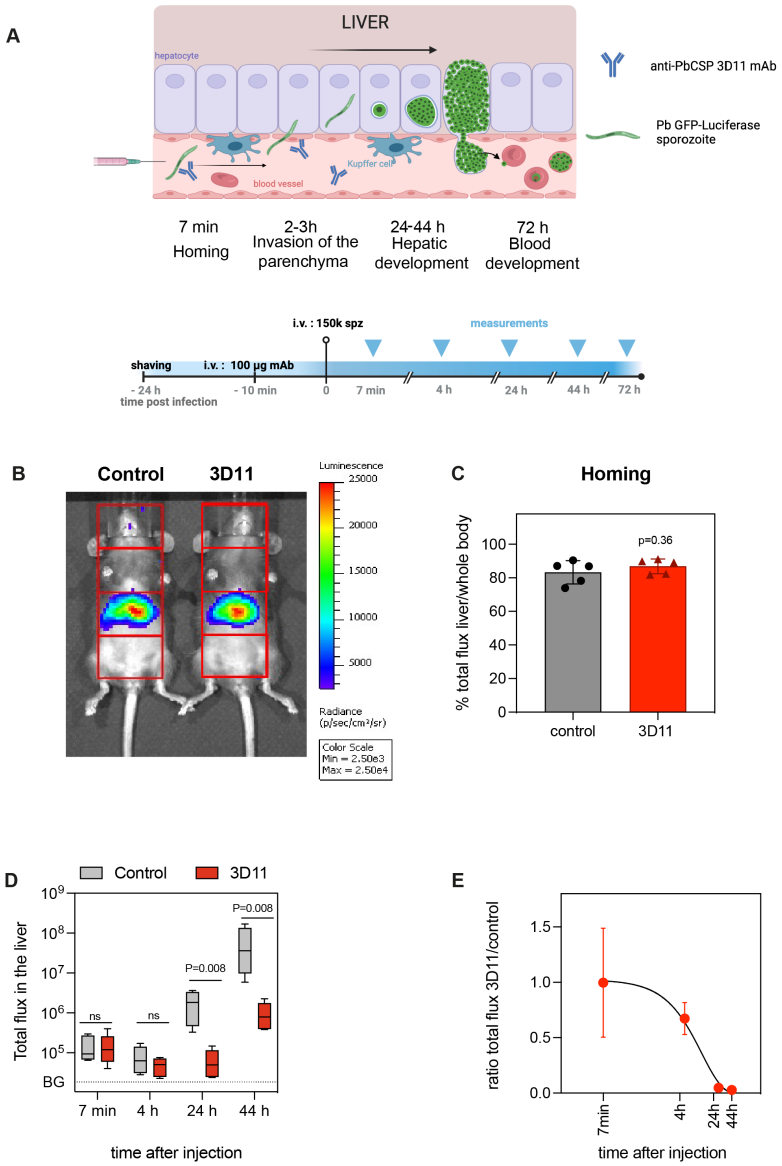

Figure 2. Kinetics of Pb sporozoite elimination in the liver. (A-E) To assess the kinetics of parasite killing by 3D11, either PBS (control) or 100 µg of 3D11 mAb were i.v. injected in mice 10-15 min before the i.v. inoculation of sporozoites expressing GFP-luciferase. Parasite load in the liver was assessed by bioluminescence. **(A) Top:** schematic representation of sporozoite homing, invasion, and development in the liver after i.v. injection. **Bottom:** representation of the experimental timing. spz: sporozoites. **(B)** Exemplary picture of the recorded bioluminescence images and define regions of interest (in red, ROIs). The signal in the 3rd quadrant was attributed to the liver. In this example, the measurement was performed 7 min after infection, the left mouse was injected with PBS while the right animal was passively transferred with 3D11. Scale in radiance (photons/sec/cm2/sr). **(C)** Quantification of the percentage of the signal collected from the liver compared to the whole body. Statistical significance was analyzed using the unpaired t-test. **(D)** Total flux (photons/s) of control and 3D11 mAb-transfered mice in the liver. Statistical significance was determined by the Multiple Mann-Whitney test. BG: background signal. **(E)** The ratio of the total flux in the liver of 3D11mAb-treated mice and control. **(C-E)** n=5 mice from 3 independent experiments. Data are presented as means ± standard deviation (SD). The cartoon was created with biorender.com.

The effect of a cytotoxic mAb on sporozoite crossing of the sinusoidal barrier

In vivo bioluminescence imaging of the liver showed that most of the parasites were eliminated by 3D11 mAb between 4 and 24 h post-i.v. inoculation. Yet, it remained unclear whether parasites

were dying in the lumen of the hepatic sinusoids or inside the hepatic parenchyma. To better observe the neutralizing mode of action of 3D11, we imaged parasites in the liver using intravital fluorescence high-speed confocal microscopy.

A titanium window was surgically inserted in the abdomen of mice [35] expressing GFP in endothelial cells [36], allowing for the longitudinal visualization of sporozoites and liver sinusoids. For these experiments, we followed the same experimental design as for the bioluminescent assay (Figure 3A). After the i.v. injection of 100 µg of 3D11, mice were anesthetized and placed on the heated stage of an inverted microscope. Similar amounts of 3D11-susceptible Pb sporozoites expressing mCherry (Pb mCherry) and non-susceptible Pb sporozoites expressing PfCSP and GFP (PbPf GFP) were then co-injected (Figure S2A) while simultaneously recording to capture the first moments of parasite arrest in the liver sinusoids [5]. Equivalent numbers of arrested susceptible (n=80) and non-susceptible (n=82) sporozoites were observed by microscopy in the analyzed fields, indicating no impairment in the ability of the parasites to stop in the liver sinusoids or die in the presence of 3D11 (Figure 3B), and confirming bioluminescence data (Figure 2C, 7 min).

Next, we quantified the inhibition of sporozoite motility by 3D11 *in vivo*. Sporozoites were scored as motile if they moved at least one body length in 5 min, otherwise, they were considered non-motile. Additionally, we also quantified if the parasites were inside the vessel or outside i.e., in the hepatic parenchyma (Figure 3C). Already 10 min after inoculation, 3D11-susceptible parasites displayed a strong impairment in motility compared to the control parasites in passively immunized mice (Figure 2B). At this time point, sporozoites were only occasionally seen dying during these first minutes, in agreement with bioluminescence data. Thirty minutes after sporozoite injection, almost none of the susceptible Pb mCherry parasites were motile while 50% of the control PbPf GFP sporozoites were still moving. Two hours later, a similar number of PbPf (n=18, Figure 3D) and Pb (n=29, Figure 3D) sporozoites were found in the liver, all, already immotile. Strikingly, only 52% of the Pb mCherry susceptible sporozoites were found in the parenchyma in contrast to 89% of non-susceptible parasites, indicating that 3D11 affects sporozoite entry into the hepatic parenchyma (Figure 3D). To exclude the fact that the insertion of the window had any effect on the results, additional experiments were performed by imaging dissected livers of passively immunized mice. *Ex vivo,* we observed that after 1 h, 97% of the control parasites (n=34) were inside the parenchyma in contrast to 53% of the susceptible sporozoites (n=45), confirming the results of the *in vivo* experiments. Since comparable numbers of Pb mCherry and PbPf GFP sporozoites were found in the microscopic fields quantified *in vivo* and *ex vivo* (Figure 3D), we can infer that 3D11 blocks sporozoite entry into the hepatic parenchyma by around 2-fold. Yet, this impairment alone cannot explain the decrease of at least one order of magnitude in the parasitemia measured 3-4 days after infection in the mice used for *in vivo* imaging (Figure S2B). Hence, in 3D11-treated mice, most sporozoites die in the hepatic parenchyma probably due to the loss of fitness caused by the cytotoxic 3D11 mAb. However, whether the late reduction in parasite load occurring after 4 h post-infection is associated with the death of extracellular sporozoites that

failed to invade hepatocytes or corresponds to the clearance of parasites undergoing abortive intracellular development couldn't be addressed *in vivo*.

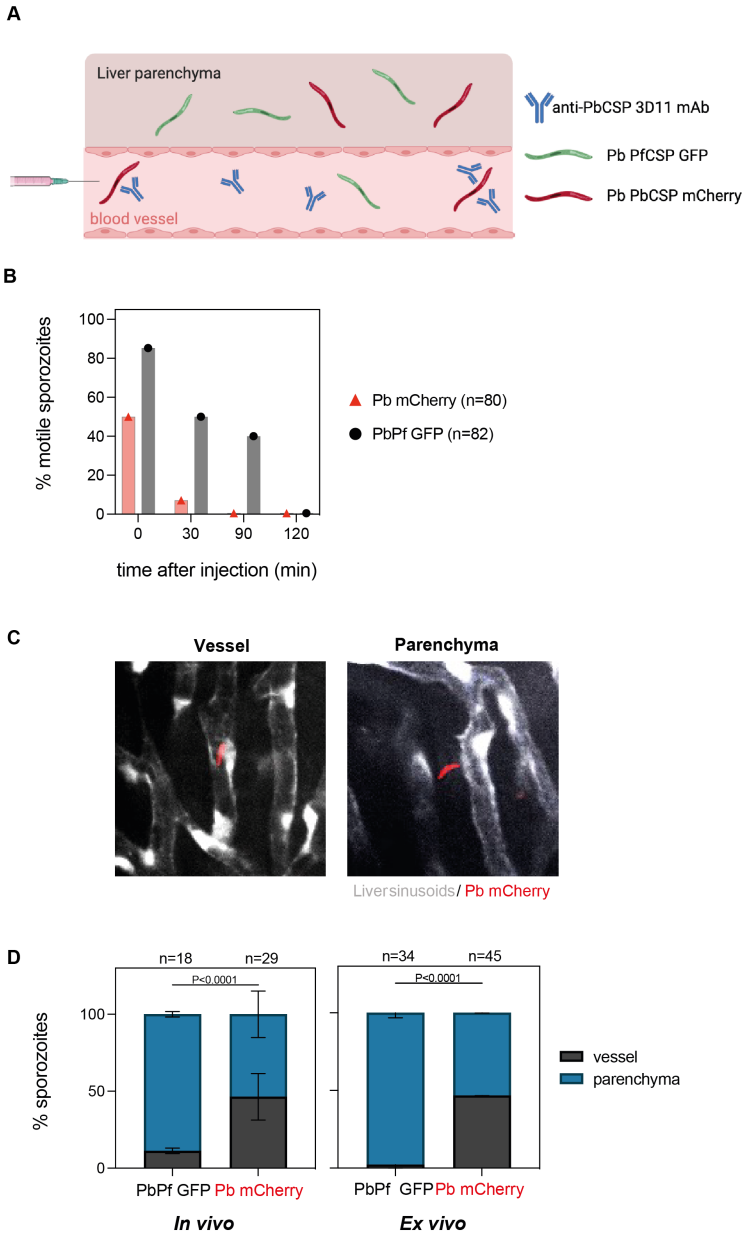

Figure 3. 3D11 inhibits sporozoite motility and partially blocks entry into the liver parenchyma. (A) Graphical representation of the experimental setup to analyze sporozoite localization in the liver. For intravital experiments (*in vivo*), flk1-GFP female mice were transferred intravenously with 100 µg of 3D11. 10 min later, the animals were placed on the microscope stage and susceptible (Pb mCherry) and control sporozoites (PbPf GFP) were co-inoculated i.v. into the tail vein. For *ex vivo* experiments, 3D11 was transferred 10 min before sporozoite injection, and 1 h later the liver was dissected and imaged. **(B)** Quantification of motility inhibition over time. Data from 4 independent experiments. **(C)** Representative images of one focal plane showing sporozoites inside the sinusoid lumen (left panel) or the hepatic parenchyma (right panel). Pb mCherry is shown in red and the GFP expressed by liver sinusoidal endothelial cells in white. **(D) Left panel:** Quantification of the localization of Pb mCherry (red) and PbPf GFP (black) sporozoites determined *in vivo* between 30 min to 3 h post-inoculation. Data from 2 independent experiments including a total of 3 animals**.** Statistical significance was determined by the Chi-square test**. Right panel:** quantification of sporozoite localization *ex vivo* determined 1 h post-inoculation. Data from two independent experiments. On top of the graphs is represented the number of quantified sporozoites. Data are presented as means ± SD. Cartoon was done with biorender.com.

In vitro effect of 3D11 on sporozoite invasion and development

To better understand the late neutralizing effect of 3D11 mAb observed on sporozoites *in vivo,* we performed an invasion and development assay *in vitro* [37] using Pb GFP-expressing sporozoites to infect the hepatoma cell line HepG2 infected, in the presence or absence of 3D11. We quantified sporozoite invasion and intracellular development by flow cytometry at 2 and 15h or 44 h post-infection, respectively. To overcome the variable invasion rates achieved across multiple experiments, the number of GFP+ cells in the cultures treated with 3D11 was normalized by the corresponding value in matching PBS-treated cultures and expressed as a percentage of control. In addition, by comparing the total number of recovered GFP+ sporozoites at 2 h in the two studied conditions, we measured the early lethality (%viable sporozoites, Figure 4B) of the anti-CSP Ab on the extracellular forms of the parasite (Figure 4A).

At 2 h, increasing concentrations of 3D11 were associated with a drastic reduction of the number of recovered extracellular sporozoites as well as a marked decrease in the percentage of GFP+ cells compared to PBS controls. 3D11 mAb therefore kills and inhibits parasite entry into cells in a dose-dependent manner (Figure 4B and 4C, 2h). Next, we compared the results of the invasion assay with 3D11-induced cytotoxicity in the same assay, expressed as a percentage of control. We summarized all the results in Figure 4B which displays a consistent pattern in the inhibition of invasion and killing. This indicates that the Ab's cytotoxic effect accounts for most of the invasion inhibition in this setting.

To determine if the cytotoxic effect of 3D11 also causes delayed killing within cells *in vitro*, we compared the percentage of surviving and developing parasites relative to the control in the 44- and 2-h time point cultures (Figure 4D). Interestingly, we observed a dose-dependent decrease in the number of intracellularly developing parasites compared to the number of invasive sporozoites, and this late effect was already reached at 15 h (Figure 4C). The dose-dependent loss of fitness caused by 3D11 mAb was also demonstrated by the decreasing GFP intensity of the remaining extraerythrocytic forms (EEFs, Figure 4E).

In line with the late neutralization effect observed *in vivo in* the liver, the *in vitro* assay demonstrates that 3D11 not only inhibits sporozoite entry into host cells but also affects its fitness resulting in subsequent parasite killing hours after invasion (Figure 2D, E).

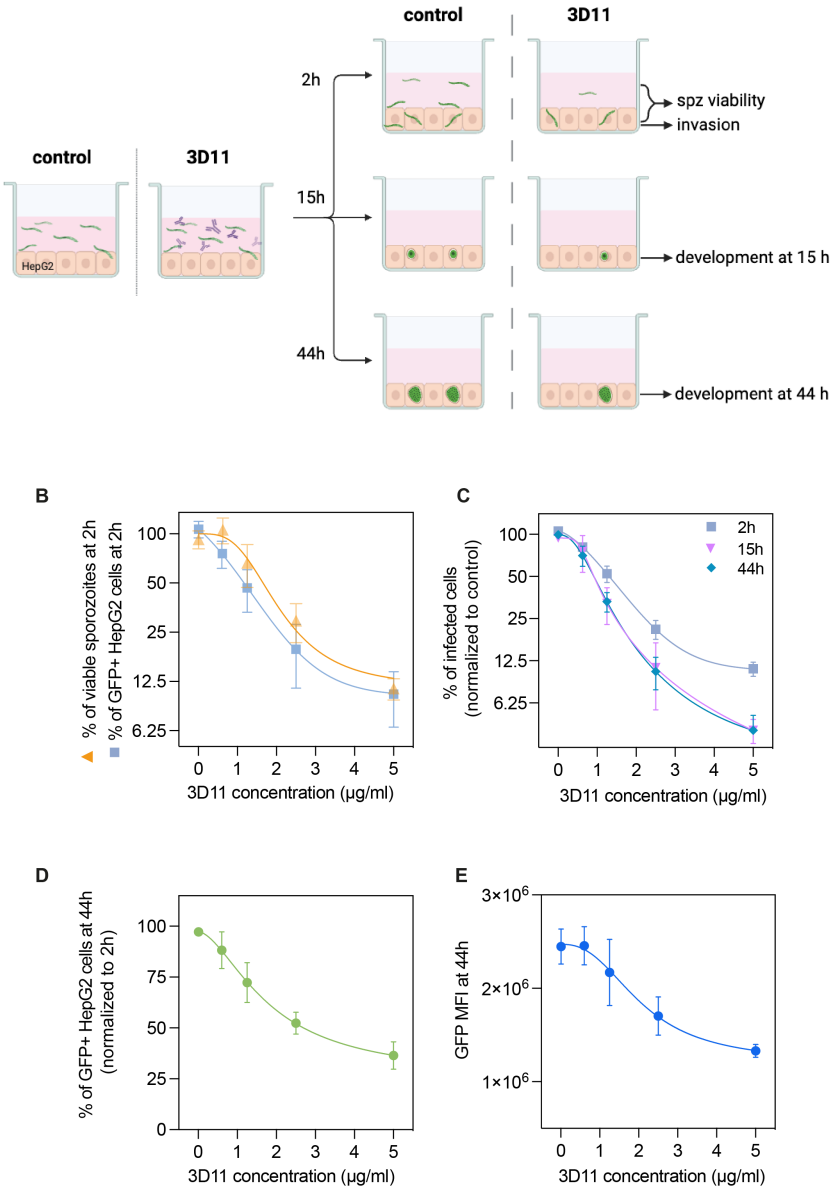

Figure 4. 3D11 inhibits sporozoite invasion and development *in vitro*. (A) Experimental setup to measure the impact of 3D11 on sporozoite invasion and EEF development in HepG2 cells. Each experiment was performed in triplicates in the presence or absence of different concentrations of 3D11. Two identical plates were prepared to assess invasion, at 2h, and development at 15 and 44h post-infection. Cells as well as the supernatant were analyzed by flow cytometry **(B)** Inhibition of HepG2 invasion by sporozoites was measured 2h after parasites were added to the culture in the presence of 3D11 (blue square). In the same assay, sporozoite viability was quantified as the percentage of viable sporozoites after 2h relative to the control (yellow triangle). **(C)** In addition to the invasion assay, development inhibition was quantified at 15 (pink inverted triangle) and 44h (blue rhombus) after sporozoite addition to the cells. **(D)** Comparison between the percentage of infected HepG2 cells at 44 and 2 h. **(E)** Mean fluorescent intensity (MFI) of EEFs 44h post-infection. **(B-E)** Data were combined from 3-4 independent experiments. Bars represent the mean ± standard error of the mean (SEM). Schema was created with biorender.com.

Discussion

The skin plays a major role in parasite-dependent cytotoxicity induced by anti-CSP Abs [4,30,31,33]. In the skin, mAbs inhibit sporozoite motility [4,30,31,33] and induce CSP shedding, leading to loss of fitness, loss of downstream infection in the liver, and sporozoite death [30,31]. However, potent mAbs can provide protection even when parasites are introduced directly into the bloodstream [31]. In the hepatic environment, these Abs have been shown to prevent parasite egress from sinusoids, hinder cell traversal, and kill sporozoites [21]. Nonetheless, it remains elusive how these effects quantitatively contribute to protection against sporozoite infection.

First of all, we verified the predominant effect of 3D11 in the skin compared to the BL by controlling the number of sporozoites for the i.v. and skin challenges, thus achieving comparable infection levels independently of the route of challenge. This allowed us to confirm that 3D11-mediated protection mainly unfolds in the skin, leading to sterile protection upon skin challenge while there is only a 10-fold decrease in parasitemia after i.v. challenge (Figure 1A). Thus, these data support the notion that 3D11 is less effective in the bloodstream [33], as higher concentrations of Abs are required to protect against i.v. challenge compared to skin challenge (Figure 1). Similarly, previous studies have reported that larger doses of 3D11 transferred to mice challenged with sporozoites via i.v. provides sterile protection [15,22].

When bioluminescent parasites are i.v. injected in passively immunized mice, 3D11 does not inhibit parasite arrest in the liver, suggesting that the repeat region of Pb CSP is not involved in sporozoite homing to the liver. It is striking that once the parasites reach the liver, the bioluminescent signal in 3D11-treated mice only decreases 30% at 4 h post-sporozoite inoculation indicating that most parasites are lately killed by 3D11. A deeper and direct analysis of parasite elimination using intravital confocal imaging of sporozoites in the liver shows that 3D11 mAb promptly inhibits parasite motility. After arresting in the liver in comparable numbers, ~80% of control PbPf sporozoites were motile, while only 40% of susceptible PbmCherry sporozoites were moving (Figure 3B). However, the reduction in motility only prevents the hepatic parenchyma invasion of ~50% of parasites. These results suggest that 3D11 inhibits sporozoite motility and limits their exit from the liver sinusoids, as previously reported [21] but this 2-fold difference in parasite translocation alone cannot completely explain the 100-fold reduction of parasitemia observed three days later in 3D11-treated versus control groups (Figure S2B). During three hours of continuous imaging, it was observed that 3D11-susceptible parasites rarely fragmented and died *in vivo*. These experiments were conducted in mice expressing GFP in endothelial cells, which made the accurate quantification of control PbPf GFP sporozoites difficult. Nonetheless, susceptible Pb mCherry parasites sporozoites were found in comparable numbers to the non-susceptible GFP sporozoites, indicating a low killing activity of 3D11 in the first 3 h post- i.v. inoculation, and in concordance with the bioluminescence experiments. This observation contrasts with the findings on the effects of potent PfCSP human monoclonal antibodies (hmAbs) where 20 and 40 % of sporozoites died while recording *in vivo* their effect in the liver [21]. This discrepancy in parasite

killing may be due to differences in Ab potency. However, this level of killing cannot also completely explain the magnitude of anti-CSP-mediated protection in both studies. To dissect the late-killing effect of the 3D11 mAb, we quantified longitudinally the *in vitro* effect of this cytotoxic antibody in the process of invasion and sporozoite development inside hepatoma HepG2 cells. As previously described, 3D11 is known to inhibit sporozoite cell invasion *in vitro*[29]. In our experimental setup, 5 µg/ml of 3D11 inhibited 88% of cell invasion (Figure 4B, C), which accounts for most of the 95% infection inhibition observed after 15 and 44 h (Figure 4C). It is important to note that the cytotoxicity of anti-CSP Abs correlates with sporozoite loss of fitness [31] , quantified by the inhibition of motility, the loss of infectivity, and the killing of sporozoites [30,31]. The dose-response similarity between the inhibition of invasion and the decrease in viability, both measured in the same assay, suggests that the inhibitory activity of 3D11 on cell invasion assays could be a consequence of the cytotoxic effect of this antibody (Figure 4B). However, this does not rule out other mechanisms of invasion inhibition. Additionally, our data also shows a late effect of 3D11 on intracellular parasites *in vitro* after Ab removal. This effect is reflected not only in the 2-fold decrease in parasite numbers between 2 h and 44 h compared to the control using 2.5 and 5 µg/ml of 3D11 (Figure 4D) but also in the decrease of EEF fitness, revealed by its decreased GFP intensity (Figure 4E). Notably, a similar effect has been previously reported using sera from mice immunized with PfCSP. Incubation of Pf sporozoites with these immune sera not only affected Pf sporozoite invasion *in vitro* but continued to affect intracellular forms for several days after invasion. Additionally, the authors of this study also observed that late EEFs from sera-treated sporozoites had abnormal morphology. Altogether, it was thus concluded that the anti-CSP Abs present in the sera had a long-term effect on the parasites [38]. Importantly, in our experimental settings and using the mAb 3D11, we didn't observe any malformation of the Pb EEFs (data not shown) but rather a decrease in the EEF GFP fluorescence at 44 h in the 3D11-treated samples compared to the control. These differences could be due to the distinct invasion and developmental process of Pb and Pf, or to the potency of the Abs present in the serum compared to 3D11. It is important to emphasize that our *in vivo* data do not suggest that 3D11 interferes with the development of surviving late EEFs, as the signal increase of survivors in 3D11-treated mice between 24, 44 and 72 h was comparable to that of control mice (Figure 2D, Figure S1). *In vitro* the late effect on EEF numbers was already reached after 15 h (Figure 3D) yet the GFP fluorescence decrease observed at 44 h (Figure 3D) could indicate that *in vitro* the cytotoxic effect might have been stronger due to the difference in concentration and time of contact between Ab and parasite.

Further experiments are needed to determine whether the parasites that invaded the hepatic parenchyma are dying, inside a parasitophorous vacuole where they are unable to develop further, trapped intracellularly during cell traversal due to the Ab inhibition of motility, or extracellularly, incapable of invading a hepatocyte as shown *in vitro*.

Although 3D11-cytotoxicity appears to be the primary contributor to the inhibition of parasite entry into the liver parenchyma *in vivo* and cell invasion *in vitro*, it is unclear whether it is the sole factor responsible for these effects. For instance, CIS43, a hmAb that targets the junctional epitope of PfCSP,

has been found to interfere with the proteolytic cleavage of CSP [16], which is a crucial process for cell invasion [39,40]. Indeed, it has recently been shown using 13 distinct PfCSP hmAbs, that protection after i.v. challenge strongly correlates with high affinity to the junctional region which contains all three repeat motifs of PfCSP (NPDP, NVDP, NANP)[31], reinforcing the hypothesis that anti-CSP repeat Abs could hinder the CSP processing at the putative cleavage site region I that is located adjacent to the junctional region of the central repetitive region of PfCSP [39]. 3D11 Fab was shown to preferentially bind to the NPND motifs that are located mostly at the junction with the N-terminal domain, but it also cross-reacts with all repeat motifs, binding to PbCSP in a spiral-like conformation [41]. Thus, further investigation is required to elucidate the role of CSP processing in the inhibition of sporozoite invasion by anti-CSP Ab, e.g., using parasites lacking the n-terminal domain of CSP [42]. To investigate other potential mechanisms by which Abs are neutralizing sporozoites in the BL, it is necessary to use non-cytotoxic conditions. This can be addressed by using a low-cytotoxic mAb, like CIS43, or parasites lacking sporozoite-secreted pore-forming proteins, such as SPECT2. It has been previously demonstrated that Ab-mediated killing is dependent on the shedding of CSP, which renders the parasite membrane susceptible to its own cell-wounding proteins [30]. According to this study, Pb and *P. yoelii* (Py) SPECT2KO mutants have a higher resistance to the killing activity of CSP Abs [30]. In conclusion, this study shows the kinetics of sporozoite elimination by the cytotoxic 3D11 mAb in the liver and quantifies the inhibitory activity of 3D11 in the key steps of hepatic infection. The measurement of the inhibition of invasion and 3D11 cytotoxicity *in vitro* suggests a potential association between these two activities. Remarkably, this study reveals a late-killing effect of cytotoxic 3D11 on sporozoites within the liver parenchyma. Anti-CSP cytotoxic Abs primarily target motile parasites in the host skin where sporozoite motility and cell traversal activity are crucial for parasite progression in the dermis as well as for Ab cytotoxicity[30–32]. Importantly, potent Abs needs to neutralize sporozoites that rapidly escape from the skin in the blood and in the liver [21,31]. This study shows that cytotoxic 3D11 mAb exerts its protective action outside the skin by inhibiting several critical steps in the hepatic infection and surprisingly, taking several hours to significantly decrease the hepatic load of parasites. Understanding the mechanisms of sporozoite neutralization by anti-CSP Abs in the host tissues is crucial for better comprehending parasite biology and developing new tools to prevent infection.

Materials and Methods

Parasites, mosquitoes and mice

For the i.v., skin, and bite challenges, we used transgenic Pb ANKA strain parasites expressing GFP (PbGFP) [43]. Pb parasites expressing GFP-luciferase (Pb GFP-luciferase) [44] were used for bioluminescence imaging. For intravital and *ex vivo* microscopy of the infected livers, Pb ANKA expressing both GFP and the full-length Pf 3D7 CSP (PbPf GFP) [21] and Pb ANKA expressing mCherry (Pb mCherry) [31] were used.

Anopheles stephensi (strain SDA 500) mosquitoes were reared at the Center for Production and Infection of Anopheles (CEPIA) at the Institut Pasteur in Paris and infected by feeding for 30 min on infected RjOrl:Swiss mice. After blood feeding the mosquitoes were maintained at 21°C with 80% humidity. Sporozoites were obtained from the salivary glands of infected mosquitoes, isolated 20-26 days after infection.

Sporozoite challenge and bioluminescence experiments were performed on female 4-week-old C57BL/6JRj mice (Janvier Labs). For intravital and *ex vivo* experiments flk1-GFP female mice aged of 5-8 weeks were used. Mice were kept in the animal facility of the CEPIA at the Institut Pasteur in Paris accredited by the French Ministry of Agriculture for performing experiments on live rodents. All experiments were performed according to French and European regulations and were approved by the Ethics Committee #89 (references MESR 01324, APAFIS#32422-2021071317049057 v2, APAFIS #32989-2021091516594748 v1).

Monoclonal antibody production and injection

3D11 anti-Pb CSP repeats IgG1 mAb was produced by an established hybridoma cell line (MRA-100, BEI Resources) [45]. W24 binds to the N-terminal domain of Py CSP and was used as an isotype control [30]. The hybridoma was cultured after the protocol of Köhler and Milstein [46]. The mAbs were isolated from the culture supernatants by affinity chromatography using Protein G beads (GE Healthcare) according to the manufacturer's instructions.

Sporozoite challenge

Abs were diluted in 1X PBS and transferred intraperitoneally 24 h before sporozoite injection or mosquito bite challenge. Mice were treated 3D11 mAb or, as control, either PBS or W24 mAb. For the skin challenge, 5,000 sporozoites were injected into the footpad of the mice using a 35G needle mounted on a NanoFil 10µl syringe (Word Precision Instruments). The i.v. challenge was performed by inoculating 1,000 sporozoites in the tail vein. Bite challenge experiments were performed using infected female *A. stephensi* mosquitoes. Mice were anesthetized using a mixture of ketamine (60 mg/kg body weight; Imalgene 1000, Merial) and xylazine (6 mg/kg body weight; 2% Rompun, Bayern. Then the mice were laid out on pots containing 10-16 mosquitoes (2 mice per pot) to be bitten for 30 minutes. The animals were rotated between the pots of each experimental group every 30-60 s.

To determine the parasitemia, a drop of blood was collected at the tip of the tail in PBS 3 to 10 days after infection. Infected red blood cells were distinguished from non-infected by detection of the fluorescence emitted by the cytoplasmic GFP of the parasite and were quantified by cytometry (CytoFLEX S, Beckman). 250,000-500,000 events were recorded.

Bioluminescence experiments

Analysis of the parasite load within animals infected with Pb expressing luciferase sporozoites was performed as previously described [5]. Briefly, the abdominal areas of 4-week-old C57BL/6JRj female mice were shaved 24 h before infection. Ten min after intravenous transfer of 100 µg of 3D11 Abs in 1x PBS, 150,000 sporozoites were i.v. injected. Immediately after parasite inoculation, mice were anesthetized with 2.5% isoflurane for two minutes. Subsequently, the animals were injected subcutaneously with 150 mg/kg body weight of D-luciferin/PBS (Perkin Elmer). After 5 minutes the signal was acquired using the IVIS® SpectrumCT (Perkin Elmer). Succeeding acquisitions were taken 4, 24, and 44 h later. For analysis, four regions of interest (ROIs) were manually defined using the Living Image®. For Figure 2F, the background noise was eliminated by subtracting from each ROI the signal obtained from the corresponding ROI applied to a non-infected mouse injected with D-luciferin.

Intravital and ex vivo microscopy

For intravital imaging, the liver of flk1-GFP mice was surgically exposed by inserting on the abdomen of the animal a titanium ring covered by a 12 mm coverslip. Twenty-four hours after the operation, the mice were injected with 3D11 Ab, anesthetized, and positioned on the microscope stage where they were injected with $0.5x10^6$ – $1x10^6$ PbPf GFP and Pb mCherry parasites (1:1 ratio). Image acquisition was started immediately after parasite injection. The time lapse between Ab and parasite injection was 10 min. For *ex vivo* experiments, no titanium window was inserted into the abdomen of the flk1-GFP mice. Ab and parasite injections were performed as described above in unanesthetized mice. 1 h after the injections, the animals were anesthetized, the liver was surgically removed, and imaged.

For intravital and *ex vivo* microscopy experiments, livers were scanned systematically and for each field, a Z-stack and a time-lapse of 5 -10 minutes were acquired over a time period for a maximum of 2-3 h after infection. Imaging was performed on a spinning-disk confocal system (UltraView ERS, PerkinElmer) controlled by Volocity (PerkinElmer) and composed of 4 Diode Pumped Solid State Lasers (excitation wavelengths: 405 nm, 488 nm, 561 nm and 640 nm), a Yokogawa Confocal Scanner Unit CSU22, a z-axis piezoelectric actuator and a Hamamatsu Orca-Flash 4.0 camera mounted on a Axiovert 200 microscope (Zeiss), using a 5–40× long-distance dry or oil-immersion objectives (Zeiss). Images were processed using Fiji [47].

In vitro invasion and development assay

Sporozoite invasion and development of the exoerythrocytic forms were quantified by flow cytometry as previously described [37]. Briefly, HepG2 cells (4×10^4 /well) were seeded in a 96-well plate and cultured overnight in DMEM (Invitrogen) supplemented with 10% heat-inactivated FCS, 1x of non-essential amino acids (Sigma) and 2% of Penicillin-Streptomycin-Neomycin (PSN) antibiotic mixture (Sigma). Uninfected and infected cells were maintained at 37°C and 5% CO_2. 10,000 PbGFP parasites were incubated with the cells (1:4 ratio) in the presence or absence of different 3D11 Ab concentrations. After 2 h, the supernatant and the trypsinized cells were analyzed by flow cytometry to quantify the amount of GFP+ events inside and outside the cells as well as the percentage of infected cells. For the samples used to analyze the development of the parasite, the cells were incubated for 15 or 44 h after sporozoite addition, the medium was changed after 2 and 24 h. The cells were trypsinized and the percentage of intracellular parasites was determined by flow cytometry.

Statistical analysis

Statistical significance was determined with a one-way ANOVA with Holm-Šídák correction for multiple comparisons, the Multiple Mann-Whitney test, paired and unpaired t-tests and the Chi-square test with the help of GraphPad Prism 10.

Author Contributions: M.C.A.-B., P.F., E.A., and R.A. conceived the project and designed experiments. M.C.A.-B., O.P., P.F., E.A., and S.C. performed experiments. E. A and M.C.A-B produced and isolated the antibodies. M.C.A.-B. wrote the manuscript. P.F., S.C., M.C.A.-B., and R.A. contributed to the manuscript revision and editing.

Funding: This research was supported by funds from the Institut Pasteur, the Agence National de la Recherche (ANR, French National Research Agency) / Deutsche Forschungsgemeinschaft (DFG, German Research Foundation) – project number SporoSTOP ANR-19-CE15-0027. M.C.A-B was funded by the Pasteur - Paris University (PPU) International Ph.D. Program.

Data Availability Statement: The data presented in this study are available upon request from the corresponding authors.

Acknowledgments: Special thanks to the team of the Center for Production and Infection of Anopheles (CEPIA, C2RA, Institut Pasteur) for providing mosquitoes and the staff of Central Animal Facility (C2RA, Institut Pasteur) for animal care and breeding. We gratefully acknowledge the UTechS Photonic BioImaging (Imagopole), C2RT, Institut Pasteur, supported by the French National Research Agency (France BioImaging; ANR-10–INBS–04; Investments for the Future « Infrastructure en Biologie et Santé.

Conflicts of Interest: The authors declare no conflict of interest. The funders had no role in the design of the study; in the collection, analyses, or interpretation of data; in the writing of the manuscript; or in the decision to publish the results.

References

(1) WHO. World Malaria Report 2023. *Geneva: World Health Organization* **2023**, Licence: CC BY-NC-SA 3.0 IGO.

(2) Vanderberg, J. P.; Sidjanski, S. Delayed Migration of Plasmodium Sporozoites from the Mosquito Bite Site to the Blood. *The American Journal of Tropical Medicine and Hygiene* **1997**, *57* (4), 426–429. https://doi.org/10.4269/ajtmh.1997.57.426.

(3) Amino, R.; Thiberge, S.; Martin, B.; Celli, S.; Shorte, S.; Frischknecht, F.; Ménard, R. Quantitative Imaging of Plasmodium Transmission from Mosquito to Mammal. *Nat Med* **2006**, *12* (2), 220–224. https://doi.org/10.1038/nm1350.

(4) Vanderberg, J. P.; Frevert, U. Intravital Microscopy Demonstrating Antibody-Mediated Immobilisation of Plasmodium Berghei Sporozoites Injected into Skin by Mosquitoes. *International Journal for Parasitology* **2004**, *34* (9), 991–996. https://doi.org/10.1016/j.ijpara.2004.05.005.

(5) Tavares, J.; Costa, D. M.; Teixeira, A. R.; Cordeiro-da-Silva, A.; Amino, R. In Vivo Imaging of Pathogen Homing to the Host Tissues. *Methods* **2017**, *127*, 37–44. https://doi.org/10.1016/j.ymeth.2017.05.008.

(6) Tavares, J.; Formaglio, P.; Thiberge, S.; Mordelet, E.; Van Rooijen, N.; Medvinsky, A.; Ménard, R.; Amino, R. Role of Host Cell Traversal by the Malaria Sporozoite during Liver Infection. *Journal of Experimental Medicine* **2013**, *210* (5), 905–915. https://doi.org/10.1084/jem.20121130.

(7) Sturm, A.; Amino, R.; Van De Sand, C.; Regen, T.; Retzlaff, S.; Rennenberg, A.; Krueger, A.; Pollok, J.-M.; Menard, R.; Heussler, V. T. Manipulation of Host Hepatocytes by the Malaria Parasite for Delivery into Liver Sinusoids. *Science* **2006**, *313* (5791), 1287–1290. https://doi.org/10.1126/science.1129720.

(8) Tarun, A. S.; Baer, K.; Dumpit, R. F.; Gray, S.; Lejarcegui, N.; Frevert, U.; Kappe, S. H. I. Quantitative Isolation and in Vivo Imaging of Malaria Parasite Liver Stages. *International Journal for Parasitology* **2006**, *36* (12), 1283–1293. https://doi.org/10.1016/j.ijpara.2006.06.009.

(9) Zavala, F.; Cochrane, A. H.; Nardin, E. H.; Nussenzweig, R. S.; Nussenzweig, V. Circumsporozoite Proteins of Malaria Parasites Contain a Single Immunodominant Region with Two or More Identical Epitopes. *The Journal of experimental medicine* **1983**, *157* (6), 1947–1957. https://doi.org/10.1084/jem.157.6.1947.

(10) Almeida, M. E. M. D.; Vasconcelos, M. G. S. D.; Tarragô, A. M.; Mariúba, L. A. M. Circumsporozoite Surface Protein-Based Malaria Vaccines: A Review. *Rev. Inst. Med. trop. S. Paulo* **2021**, *63*, e11. https://doi.org/10.1590/s1678-9946202163011.

(11) White, M. T.; Bejon, P.; Olotu, A.; Griffin, J. T.; Bojang, K.; Lusingu, J.; Salim, N.; Abdulla, S.; Otsyula, N.; Agnandji, S. T.; Lell, B.; Asante, K. P.; Owusu-Agyei, S.; Mahama, E.; Agbenyega, T.; Ansong, D.; Sacarlal, J.; Aponte, J. J.; Ghani, A. C. A Combined Analysis of Immunogenicity, Antibody Kinetics and Vaccine Efficacy from Phase 2 Trials of the RTS,S Malaria Vaccine. *BMC Med* **2014**, *12* (1), 117. https://doi.org/10.1186/s12916-014-0117-2.

(12) White, M. T.; Bejon, P.; Olotu, A.; Griffin, J. T.; Riley, E. M.; Kester, K. E.; Ockenhouse, C. F.; Ghani, A. C. The Relationship between RTS,S Vaccine-Induced Antibodies, CD4+ T Cell Responses and Protection against

Plasmodium Falciparum Infection. *PLoS ONE* **2013**, *8* (4), e61395. https://doi.org/10.1371/journal.pone.0061395.

(13) White, M. T.; Verity, R.; Griffin, J. T.; Asante, K. P.; Owusu-Agyei, S.; Greenwood, B.; Drakeley, C.; Gesase, S.; Lusingu, J.; Ansong, D.; Adjei, S.; Agbenyega, T.; Ogutu, B.; Otieno, L.; Otieno, W.; Agnandji, S. T.; Lell, B.; Kremsner, P.; Hoffman, I.; Martinson, F.; Kamthunzu, P.; Tinto, H.; Valea, I.; Sorgho, H.; Oneko, M.; Otieno, K.; Hamel, M. J.; Salim, N.; Mtoro, A.; Abdulla, S.; Aide, P.; Sacarlal, J.; Aponte, J. J.; Njuguna, P.; Marsh, K.; Bejon, P.; Riley, E. M.; Ghani, A. C. Immunogenicity of the RTS,S/AS01 Malaria Vaccine and Implications for Duration of Vaccine Efficacy: Secondary Analysis of Data from a Phase 3 Randomised Controlled Trial. *The Lancet Infectious Diseases* **2015**, *15* (12), 1450–1458. https://doi.org/10.1016/S1473-3099(15)00239-X.

(14) Yoshida, N.; Nussenzweig, R. S.; Potocnjak, P.; Nussenzweig, V.; Aikawa, M. Hybridoma Produces Protective Antibodies Directed Against the Sporozoite Stage of Malaria Parasite. *Science* **1980**, *207* (4426), 71–73. https://doi.org/10.1126/science.6985745.

(15) Potocnjak, P.; Yoshida, N.; Nussenzweig, R. S.; Nussenzweig, V. Monovalent Fragments (Fab) of Monoclonal Antibodies to a Sporozoite Surface Antigen (Pb44) Protect Mice against Malarial Infection. *Journal of Experimental Medicine* **1980**, *151* (6), 1504–1513. https://doi.org/10.1084/jem.151.6.1504.

(16) Kisalu, N. K.; Idris, A. H.; Weidle, C.; Flores-Garcia, Y.; Flynn, B. J.; Sack, B. K.; Murphy, S.; Schön, A.; Freire, E.; Francica, J. R.; Miller, A. B.; Gregory, J.; March, S.; Liao, H.-X.; Haynes, B. F.; Wiehe, K.; Trama, A. M.; Saunders, K. O.; Gladden, M. A.; Monroe, A.; Bonsignori, M.; Kanekiyo, M.; Wheatley, A. K.; McDermott, A. B.; Farney, S. K.; Chuang, G.-Y.; Zhang, B.; Kc, N.; Chakravarty, S.; Kwong, P. D.; Sinnis, P.; Bhatia, S. N.; Kappe, S. H. I.; Sim, B. K. L.; Hoffman, S. L.; Zavala, F.; Pancera, M.; Seder, R. A. A Human Monoclonal Antibody Prevents Malaria Infection by Targeting a New Site of Vulnerability on the Parasite. *Nat Med* **2018**, *24* (4), 408–416. https://doi.org/10.1038/nm.4512.

(17) Oyen, D.; Torres, J. L.; Wille-Reece, U.; Ockenhouse, C. F.; Emerling, D.; Glanville, J.; Volkmuth, W.; Flores-Garcia, Y.; Zavala, F.; Ward, A. B.; King, C. R.; Wilson, I. A. Structural Basis for Antibody Recognition of the NANP Repeats in *Plasmodium Falciparum* Circumsporozoite Protein. *Proc. Natl. Acad. Sci. U.S.A.* **2017**, *114* (48). https://doi.org/10.1073/pnas.1715812114.

(18) Imkeller, K.; Scally, S. W.; Bosch, A.; Martí, G. P.; Costa, G.; Triller, G.; Murugan, R.; Renna, V.; Jumaa, H.; Kremsner, P. G.; Sim, B. K. L.; Hoffman, S. L.; Mordmüller, B.; Levashina, E. A.; Julien, J.-P.; Wardemann, H. Antihomotypic Affinity Maturation Improves Human B Cell Responses against a Repetitive Epitope. *Science* **2018**, *360* (6395), 1358–1362. https://doi.org/10.1126/science.aar5304.

(19) Tan, J.; Sack, B. K.; Oyen, D.; Zenklusen, I.; Piccoli, L.; Barbieri, S.; Foglierini, M.; Fregni, C. S.; Marcandalli, J.; Jongo, S.; Abdulla, S.; Perez, L.; Corradin, G.; Varani, L.; Sallusto, F.; Sim, B. K. L.; Hoffman, S. L.; Kappe, S. H. I.; Daubenberger, C.; Wilson, I. A.; Lanzavecchia, A. A Public Antibody Lineage That Potently Inhibits Malaria Infection through Dual Binding to the Circumsporozoite Protein. *Nat Med* **2018**, *24* (4), 401–407. https://doi.org/10.1038/nm.4513.

(20) Murugan, R.; Buchauer, L.; Triller, G.; Kreschel, C.; Costa, G.; Pidelaserra Martí, G.; Imkeller, K.; Busse, C. E.; Chakravarty, S.; Sim, B. K. L.; Hoffman, S. L.; Levashina, E. A.; Kremsner, P. G.; Mordmüller, B.; Höfer, T.; Wardemann, H. Clonal Selection Drives Protective Memory B Cell Responses in Controlled Human Malaria Infection. *Sci. Immunol.* **2018**, *3* (20), eaap8029. https://doi.org/10.1126/sciimmunol.aap8029.

(21) Wang, L. T.; Pereira, L. S.; Flores-Garcia, Y.; O'Connor, J.; Flynn, B. J.; Schön, A.; Hurlburt, N. K.; Dillon,

M.; Yang, A. S. P.; Fabra-García, A.; Idris, A. H.; Mayer, B. T.; Gerber, M. W.; Gottardo, R.; Mason, R. D.; Cavett, N.; Ballard, R. B.; Kisalu, N. K.; Molina-Cruz, A.; Nelson, J.; Vistein, R.; Barillas-Mury, C.; Amino, R.; Baker, D.; King, N. P.; Sauerwein, R. W.; Pancera, M.; Cockburn, I. A.; Zavala, F.; Francica, J. R.; Seder, R. A. A Potent Anti-Malarial Human Monoclonal Antibody Targets Circumsporozoite Protein Minor Repeats and Neutralizes Sporozoites in the Liver. *Immunity* **2020**, *53* (4), 733-744.e8. https://doi.org/10.1016/j.immuni.2020.08.014.

(22) Charoenvit, Y.; Mellouk, S.; Cole, C.; Bechara, R.; Leef, M. F.; Sedegah, M.; Yuan, L. F.; Robey, F. A.; Beaudoin, R. L.; Hoffman, S. L. Monoclonal, but Not Polyclonal, Antibodies Protect against Plasmodium Yoelii Sporozoites. *J Immunol* **1991**, *146* (3), 1020–1025.

(23) Cochrane, A. H.; Santoro, F.; Nussenzweig, V.; Gwadz, R. W.; Nussenzweig, R. S. Monoclonal Antibodies Identify the Protective Antigens of Sporozoites of Plasmodium Knowlesi. *Proc Natl Acad Sci U S A* **1982**, *79* (18), 5651–5655. https://doi.org/10.1073/pnas.79.18.5651.

(24) Gaudinski, M. R.; Berkowitz, N. M.; Idris, A. H.; Coates, E. E.; Holman, L. A.; Mendoza, F.; Gordon, I. J.; Plummer, S. H.; Trofymenko, O.; Hu, Z.; Campos Chagas, A.; O'Connell, S.; Basappa, M.; Douek, N.; Narpala, S. R.; Barry, C. R.; Widge, A. T.; Hicks, R.; Awan, S. F.; Wu, R. L.; Hickman, S.; Wycuff, D.; Stein, J. A.; Case, C.; Evans, B. P.; Carlton, K.; Gall, J. G.; Vazquez, S.; Flach, B.; Chen, G. L.; Francica, J. R.; Flynn, B. J.; Kisalu, N. K.; Capparelli, E. V.; McDermott, A.; Mascola, J. R.; Ledgerwood, J. E.; Seder, R. A. A Monoclonal Antibody for Malaria Prevention. *N Engl J Med* **2021**, *385* (9), 803–814. https://doi.org/10.1056/NEJMoa2034031.

(25) Kayentao, K.; Ongoiba, A.; Preston, A. C.; Healy, S. A.; Doumbo, S.; Doumtabe, D.; Traore, A.; Traore, H.; Djiguiba, A.; Li, S.; Peterson, M. E.; Telscher, S.; Idris, A. H.; Kisalu, N. K.; Carlton, K.; Serebryannyy, L.; Narpala, S.; McDermott, A. B.; Gaudinski, M.; Traore, S.; Cisse, H.; Keita, M.; Skinner, J.; Hu, Z.; Zéguimé, A.; Ouattara, A.; Doucoure, M.; Dolo, A.; Djimdé, A.; Traore, B.; Seder, R. A.; Crompton, P. D. Safety and Efficacy of a Monoclonal Antibody against Malaria in Mali. *N Engl J Med* **2022**, *387* (20), 1833–1842. https://doi.org/10.1056/NEJMoa2206966.

(26) Wu, R. L.; Idris, A. H.; Berkowitz, N. M.; Happe, M.; Gaudinski, M. R.; Buettner, C.; Strom, L.; Awan, S. F.; Holman, L. A.; Mendoza, F.; Gordon, I. J.; Hu, Z.; Campos Chagas, A.; Wang, L. T.; Da Silva Pereira, L.; Francica, J. R.; Kisalu, N. K.; Flynn, B. J.; Shi, W.; Kong, W.-P.; O'Connell, S.; Plummer, S. H.; Beck, A.; McDermott, A.; Narpala, S. R.; Serebryannyy, L.; Castro, M.; Silva, R.; Imam, M.; Pittman, I.; Hickman, S. P.; McDougal, A. J.; Lukoskie, A. E.; Murphy, J. R.; Gall, J. G.; Carlton, K.; Morgan, P.; Seo, E.; Stein, J. A.; Vazquez, S.; Telscher, S.; Capparelli, E. V.; Coates, E. E.; Mascola, J. R.; Ledgerwood, J. E.; Dropulic, L. K.; Seder, R. A. Low-Dose Subcutaneous or Intravenous Monoclonal Antibody to Prevent Malaria. *N Engl J Med* **2022**, *387* (5), 397–407. https://doi.org/10.1056/NEJMoa2203067.

(27) Stewart, M. J.; Vanderberg, J. P. Malaria Sporozoites Release Circumsporozoite Protein from Their Apical End and Translocate It along Their Surface. *The Journal of Protozoology* **1991**, *38* (4), 411–421. https://doi.org/10.1111/j.1550-7408.1991.tb01379.x.

(28) Stewart, M. J.; Nawrot, R. J.; Schulman, S.; Vanderberg, J. P. Plasmodium Berghei Sporozoite Invasion Is Blocked in Vitro by Sporozoite-Immobilizing Antibodies. *Infect Immun* **1986**, *51* (3), 859–864. https://doi.org/10.1128/iai.51.3.859-864.1986.

(29) Hollingdale, M. R.; Zavala, F.; Nussenzweig, R. S.; Nussenzweig, V. Antibodies to the Protective Antigen of Plasmodium Berghei Sporozoites Prevent Entry into Cultured Cells. *J Immunol* **1982**, *128* (4), 1929–1930.

(30) Aliprandini, E.; Tavares, J.; Panatieri, R. H.; Thiberge, S.; Yamamoto, M. M.; Silvie, O.; Ishino, T.; Yuda, M.; Dartevelle, S.; Traincard, F.; Boscardin, S. B.; Amino, R. Cytotoxic Anti-Circumsporozoite Antibodies Target Malaria Sporozoites in the Host Skin. *Nat Microbiol* **2018**, *3* (11), 1224–1233. https://doi.org/10.1038/s41564-018-0254-z.

(31) Aguirre-Botero, M. C.; Wang, L. T.; Formaglio, P.; Aliprandini, E.; Thiberge, J.-M.; Schön, A.; Flores-Garcia, Y.; Mathis-Torres, S.; Flynn, B. J.; Da Silva Pereira, L.; Le Duff, Y.; Hurley, M.; Nacer, A.; Bowyer, P. W.; Zavala, F.; Idris, A. H.; Francica, J. R.; Seder, R. A.; Amino, R. Cytotoxicity of Human Antibodies Targeting the Circumsporozoite Protein Is Amplified by 3D Substrate and Correlates with Protection. *Cell Reports* **2023**, *42* (7), 112681. https://doi.org/10.1016/j.celrep.2023.112681.

(32) Amino, R.; Giovannini, D.; Thiberge, S.; Gueirard, P.; Boisson, B.; Dubremetz, J.-F.; Prévost, M.-C.; Ishino, T.; Yuda, M.; Ménard, R. Host Cell Traversal Is Important for Progression of the Malaria Parasite through the Dermis to the Liver. *Cell Host & Microbe* **2008**, *3* (2), 88–96. https://doi.org/10.1016/j.chom.2007.12.007.

(33) Flores-Garcia, Y.; Nasir, G.; Hopp, C. S.; Munoz, C.; Balaban, A. E.; Zavala, F.; Sinnis, P. Antibody-Mediated Protection against *Plasmodium* Sporozoites Begins at the Dermal Inoculation Site. *mBio* **2018**, *9* (6), e02194-18. https://doi.org/10.1128/mBio.02194-18.

(34) Mathieu, C.; Demarta-Gatsi, C.; Porcherie, A.; Brega, S.; Thiberge, S.; Ronce, K.; Smith, L.; Peronet, R.; Amino, R.; Ménard, R.; Mécheri, S. Plasmodium Berghei Histamine-Releasing Factor Favours Liver-Stage Development via Inhibition of IL-6 Production and Associates with a Severe Outcome of Disease. *Cell Microbiol* **2015**, *17* (4), 542–558. https://doi.org/10.1111/cmi.12382.

(35) Ritsma, L.; Steller, E. J. A.; Ellenbroek, S. I. J.; Kranenburg, O.; Borel Rinkes, I. H. M.; van Rheenen, J. Surgical Implantation of an Abdominal Imaging Window for Intravital Microscopy. *Nat Protoc* **2013**, *8* (3), 583–594. https://doi.org/10.1038/nprot.2013.026.

(36) Xu, Y.; Yuan, L.; Mak, J.; Pardanaud, L.; Caunt, M.; Kasman, I.; Larrivée, B.; Del Toro, R.; Suchting, S.; Medvinsky, A.; Silva, J.; Yang, J.; Thomas, J.-L.; Koch, A. W.; Alitalo, K.; Eichmann, A.; Bagri, A. Neuropilin-2 Mediates VEGF-C–Induced Lymphatic Sprouting Together with VEGFR3. *Journal of Cell Biology* **2010**, *188* (1), 115–130. https://doi.org/10.1083/jcb.200903137.

(37) Prudêncio, M.; Rodrigues, C. D.; Ataíde, R.; Mota, M. M. Dissecting in Vitro Host Cell Infection by Plasmodium Sporozoites Using Flow Cytometry. *Cell Microbiol* **2007**, *0* (0), 070816152918001-??? https://doi.org/10.1111/j.1462-5822.2007.01032.x.

(38) Mazier, D.; Mellouk, S.; Beaudoin, R. L.; Texier, B.; Druilhe, P.; Hockmeyer, W.; Trosper, J.; Paul, C.; Charoenvit, Y.; Young, J. Effect of Antibodies to Recombinant and Synthetic Peptides on P. Falciparum Sporozoites in Vitro. *Science* **1986**, *231* (4734), 156–159. https://doi.org/10.1126/science.3510455.

(39) Coppi, A.; Pinzon-Ortiz, C.; Hutter, C.; Sinnis, P. The Plasmodium Circumsporozoite Protein Is Proteolytically Processed during Cell Invasion. *Journal of Experimental Medicine* **2005**, *201* (1), 27–33. https://doi.org/10.1084/jem.20040989.

(40) Espinosa, D. A.; Gutierrez, G. M.; Rojas-López, M.; Noe, A. R.; Shi, L.; Tse, S.-W.; Sinnis, P.; Zavala, F. Proteolytic Cleavage of the *Plasmodium Falciparum* Circumsporozoite Protein Is a Target of Protective Antibodies. *J Infect Dis.* **2015**, *212* (7), 1111–1119. https://doi.org/10.1093/infdis/jiv154.

(41) Kucharska, I.; Thai, E.; Srivastava, A.; Rubinstein, J. L.; Pomès, R.; Julien, J.-P. Structural Ordering of the Plasmodium Berghei Circumsporozoite Protein Repeats by Inhibitory Antibody 3D11. *eLife* **2020**, *9*, e59018. https://doi.org/10.7554/eLife.59018.

(42) Coppi, A.; Natarajan, R.; Pradel, G.; Bennett, B. L.; James, E. R.; Roggero, M. A.; Corradin, G.; Persson, C.; Tewari, R.; Sinnis, P. The Malaria Circumsporozoite Protein Has Two Functional Domains, Each with Distinct Roles as Sporozoites Journey from Mosquito to Mammalian Host. *Journal of Experimental Medicine* **2011**, *208* (2), 341–356. https://doi.org/10.1084/jem.20101488.

(43) Ishino, T.; Orito, Y.; Chinzei, Y.; Yuda, M. A Calcium-dependent Protein Kinase Regulates *Plasmodium* Ookinete Access to the Midgut Epithelial Cell. *Molecular Microbiology* **2006**, *59* (4), 1175–1184. https://doi.org/10.1111/j.1365-2958.2005.05014.x.

(44) Flores-Garcia, Y.; Herrera, S. M.; Jhun, H.; Pérez-Ramos, D. W.; King, C. R.; Locke, E.; Raghunandan, R.; Zavala, F. Optimization of an in Vivo Model to Study Immunity to Plasmodium Falciparum Pre-Erythrocytic Stages. *Malar J* **2019**, *18* (1), 426. https://doi.org/10.1186/s12936-019-3055-9.

(45) Eichinger, D. J.; Arnot, D. E.; Tam, J. P.; Nussenzweig, V.; Enea, V. Circumsporozoite Protein of Plasmodium Berghei: Gene Cloning and Identification of the Immunodominant Epitopes. *Mol. Cell. Biol.* **1986**, *6* (11), 3965–3972. https://doi.org/10.1128/MCB.6.11.3965.

(46) Köhler, G.; Milstein, C. Continuous Cultures of Fused Cells Secreting Antibody of Predefined Specificity. *Nature* **1975**, *256* (5517), 495–497. https://doi.org/10.1038/256495a0.

(47) Schindelin, J.; Arganda-Carreras, I.; Frise, E.; Kaynig, V.; Longair, M.; Pietzsch, T.; Preibisch, S.; Rueden, C.; Saalfeld, S.; Schmid, B.; Tinevez, J.-Y.; White, D. J.; Hartenstein, V.; Eliceiri, K.; Tomancak, P.; Cardona, A. Fiji: An Open-Source Platform for Biological-Image Analysis. *Nat Methods* **2012**, *9* (7), 676–682. https://doi.org/10.1038/nmeth.2019.

Supplementary data

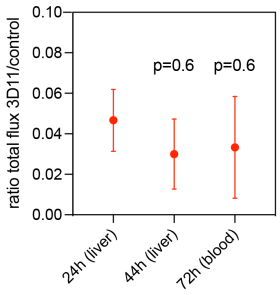

Figure S1. Comparison of the ratio of total flux between 3D11-treated and control mice 14, 44, and 72 h post-infection (n= 3 animals). The analyzed ROI at 24 and 44 h was located in the upper abdominal region while at 72 h we analyzed the signal of the whole body since at this time point the parasites are outside the liver and have invaded the erythrocytes. Statistical significance was determined by the Multiple Mann-Whitney test. BG: background signal. Data are presented as means ± SD.

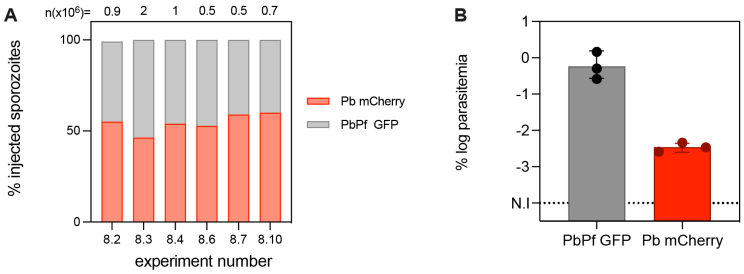

Figure S2. (A) The total amount of sporozoites as well as the percentage of Pb mCherry or PbPf GFP sporozoites that were injected in each experiment in Figure 3. 8.2,8.3, 8.4, 8.6: motility analysis. 8.2, 8.3: intravital imagining experiments. 8.7 and 8.10: *ex vivo* imaging. **(B)** log percentage parasitemia of mice used for intravital imaging experiments 3 days after sporozoites injection. Statistical significance was determined using the paired t-test.